Meteorology and Atmospheric Physics (2022) 134:9
https://doi.org/10.1007/s00703-021-00845-7

ORIGINAL PAPER

Simulation of an extreme rainfall event over Mumbai using a regional climate model: a case study

Manas Pant[1,2] · Soumik Ghosh[1,3] · Shruti Verma[1] · Palash Sinha[4] · R. K. Mall[2] · R. Bhatla[1,2]

Received: 25 September 2020 / Accepted: 4 November 2021 / Published online: 25 November 2021

Abstract

An endeavor has been made to utilize the ICTP's regional climate model RegCM for simulating one of the most catastrophic rainfall events recorded in the history of Mumbai, India on 26th July 2005. The recent version of the model, i.e., RegCM4.6 has been used to dynamically downscale this extreme event at 25 km horizontal resolution over the South-Asia Coordinated Regional Climate Downscaling Experiment (SA-CORDEX) domain with initial and lateral boundary conditions from ERA-Interim reanalysis (EIN15). Due to the coarse resolution of the EIN15, the rainfall pattern during the extreme rainfall event that occurred over Mumbai is fairly unviable. However, the implementation of the dynamical downscaling using RegCM4.6 successfully able to capture the extreme events. The results indicate the RegCM4.6 using mixed cumulus parameterization scheme (CPS; where the Emanuel scheme is considered over land and the Grell scheme is forced over ocean (EL_GO) capable of downscaling the heavy rainfall event with higher accuracy compared to forcing data. This highly confined event over Mumbai might be a manifestation of the low-pressure area formed over Orissa and the adjoining regions associated with mid-tropospheric cyclonic (MTC) circulation over the western coastal region. A detailed analysis suggests that the RegCM4.6 is able to reproduce the localized event satisfactorily as far as the spatial and temporal aspects are concerned. There is a significant improvement in the model simulated output closer to the observations in terms of qualitative and quantitative analysis of rainfall and large-scale fields. Furthermore, the RegCM satisfactorily simulates the features such as the convergence at the lower level accompanied with the divergence at the upper level, higher cyclonic vorticity near lower level, and presence of an enormous amount of moisture content at different pressure levels.

1 Introduction

The Indian Agriculture, economy, and social aspects are emphatically dependent upon the southwest monsoon. The Indian subcontinent receives about 80% of its annual rainfall during the season which lasts over the country from June, July, August, and September (JJAS). The Indian Summer Monsoon (ISM) is often associated with heavy to extremely heavy rainfall (Rajeevan et al. 2006). Some studies have shown that the variability of the ISM has been reinforced in recent few decades (Ghosh et al. 2012; Singh et al. 2014) and the regular pattern of ISM rainfall is being affected (Turner and Annamalai 2012; Roxy et al. 2017). A rising tendency in the number and intensity of extreme rainfall events has been observed over the Indian subcontinent (Goswami et al. 2006; Guhathakurta et al. 2011; Swain et al. 2019a).

The core monsoon regions (central Indian region) are vulnerable due to the heavy rainfall events, flash floods, and landslides which cause loss of lives and badly affect the socio-economic aspects (Revadekar and Preethi2012). In a study, Roxy et al. (2017) have shown a threefold increase in rainfall extremes over central India during 1950–2015 and manifest the enhanced vagaries of monsoon westerlies over the Arabian Sea. The variability of ISM causes temporal or spatial variations, and the pattern of rainfall can lead to drought or excessive flood over the

Communicated by Stephanie Fiedler.

✉ R. Bhatla
rbhatla@bhu.ac.in

[1] Department of Geophysics, Institute of Science, Banaras Hindu University, Varanasi, India

[2] DST-Mahamana Centre of Excellence in Climate Change Research, Institute of Environment and Sustainable Development, Banaras Hindu University, Varanasi, India

[3] Present Address: Department of Earth and Planetary Sciences, Weizmann Institute of Science, Revovot, Israel

[4] School of Earth, Ocean and Climate Sciences, Indian Institute of Technology, Bhubaneshwar, Orissa, India

Indian region which adversely affects the socio-economy of the country (Das et al. 2007; Simpkins 2017). The study by Almazroui et al. (2020) has proposed a significant increase in projected temperature and precipitation over South Asia and Indian subcontinent regions during the summer monsoon season. Rainfall during the monsoon season is based on the southwesterly flow of wind which is influenced by the depression over the Arabian Sea and the Bay of Bengal (BOB) (Krishnamurthy and Shukla 2007). However, Nikumbh et al. (2020) have shown, only a strong low-pressure system or depression is not sufficient to produce large-scale extreme rainfall events. However, the low-pressure systems along with secondary cyclonic vorticity may intensify the dynamic lifting of rising air and moisture transport from the Arabian Sea (Swain et al. 2019b). Using the regional climate model, Sinha et al. (2014) and Ashfaq (2020) found that the South Asia topography plays a vital role in regulating the monsoon circulation as it helps to hold the conducive environment for the monsoon precipitation. Ogura and Yoshizaki (1988) have discovered that the elevation of the Western Ghat is one of the main factors for deep convection well offshore over the Arabian Sea. The mountainous zone works as a barrier for monsoon wind which sometimes causes heavy to extremely heavy rainfall over and nearby region (Soman and Krishnakumar 1990; Smith 1985). Studies of Krishnamurti and Hawkins (1970) and Benson and Rao (1987) have suggested that the mid-tropospheric cyclone (MTC) and convection in tropical convergence zone are also major factors that are responsible for the extremely heavy rainfall over the Western Ghats and adjoining regions. A detailed description of MTC can be found in Miller and Keshavamurthy (1967). As per India Meteorological Department (IMD), rainfall amount of 6.5–12.4 cm within 24 h is termed as heavy rainfall, 12.4–24.4 cm as very heavy rainfall and if it exceeds 24.4 cm it is termed as extremely heavy rainfall (DST 2001). However, in general, the west coast and nearby regions receive 10–300 mm of rainfall per day during the southwest monsoon season (Vaidya and Kulkarni 2007) but some extreme rainfall events (~ 500 mm) have been reported in the past (Rakhecha et al. 1990; Dhar and Nandargi 1998) over these regions. Some of the extreme rainfall events such as 375 mm of rainfall on July 5th, 1975, 318 mm on September 23rd, 1981, 399 mm on June 10th, 1991, and 346 mm on August 23rd, 1997 occurred over the surrounded regions of Western Ghats and Mumbai (Jenamani et al. 2006). In August 2018, 440 people were found dead due to the flood over Kerala because of the extreme rainfall (Gulf News 30th August 2018). The study of Mishra et al. (2018) showed that the respective catastrophic flood over Kerala occurred due to multi-day extreme precipitation, and the orography is one of the major reasons to enhancing the severity of the extreme (Baisya and Pattnaik 2019).

On 26th July 2005, life in Mumbai city became standstill and Santacruz meteorological station operated by Govt. of India recorded 944.2 mm of rainfall in 24 h. Some nearby places were also experienced heavy rainfall events. However, observatory at Colaba, situated within 24 km in the south of Santacruz observatory had recorded very less amount of rainfall (73 mm) during the same period. It indicates that extremely heavy rainfall event in Mumbai is highly localized. Bohra et al. (2006) have found a significant increase in rainfall of 80 mm in south Mumbai using the National Centre for Medium Range Weather Forecasting (NCMRWF) high-resolution global model. Jenamani et al. (2006) have made an attempt to find out the thermodynamical aspects to find the possible cause behind the occurrence of the Mumbai rainfall event. They identified that the lower level moisture flows from the Arabian Sea and the dry air in mid-tropospheric levels causes an enhancement of the thunderstorm over the region. By combining the satellite and radar input with synoptic and thermodynamic features, Shyamala and Bhadram (2006) have found that the formation of the super thunderstorm triggered the heavy rainfall over the region. Furthermore, they concluded that the extreme rainfall episode over Mumbai is a manifestation of the interaction between mesoscale and synoptic scale. In another modelling study with Fifth-Generation National Center for Atmospheric Research (NCAR)/Penn State Mesoscale Model (MM5), Litta et al. (2007) have proposed that the amount and the location of rainfall are very sensitive on appropriate cumulus parameterization scheme (CPS). Their study finds the Grell scheme as the best performing scheme to study rainfall extremes. They have also explained that the formation of the mid-tropospheric mesoscale vortices and the active monsoon phase over the western coastal region causes the heavy rainfall for the respective event. Vaidya and Kulkarni (2007) find a need of three-dimensional cloud model to study such kind of extreme rainfall events as the advanced regional prediction system model has a poor skill to simulate the 381 mm rainfall during 09 UTC to 12 UTC on July 26th, 2005. Study with Weather Research and Forecast (WRF) model propose that the strong large-scale rising in the atmospheric circulation is occurred due to the enhancement in the land-sea heating and topography of Western Ghats (Kumar et al. 2008). The data assimilation techniques improve the performance of the WRF model in simulating extreme rainfall events along with the associate thermodynamic (Mohanty et al. 2012). Dodla and Ratna (2010) have studied the Mumbai rainfall event using the high-resolution NCAR/MM5 model and have demonstrated the benefit of four-dimensional data assimilation (FDDA) nudging technique for predicting more precisely the location and intensity of rainfall. Their experiment is able to

produce 550 mm of rainfall within 24 h as the interaction of the synoptic and mesoscale circulation causes the extreme rainfall event. The deep convection process is governed by the cyclonic circulation in mid-troposphere, which extended towards the lower level during the later stages of the event (Sahany et al. 2010). An earlier study has revealed the pattern and relative mechanism on the synoptic and mesoscale regarding the formation and growth of heavy rainfall events in the model simulation (Schwartz et al. 1990). The high-resolution mesoscale model has the ability to simulate or forecast severe weather conditions (Kumar et al. 2008) with limited forecast skills of 2–3 days (Sikka and Rao 2008; Das et al. 2008). Winkler (1988) has attempted the prediction of a summer-time rainfall extreme and has proposed that the improvement in the regional climate model (RCM) is helpful to understand the climatological features of extreme rainfall events. It has the efficiency to simulate the atmospheric states with a higher skill beyond a larger time scale, such as monthly and seasonal scale (Xue et al. 2014; Saeed et al. 2006, 2011). Though, the dynamical downscaling over a smaller region or sub-region is still a challenge for the climate modelers. For this purpose, RCM by ICTP, Italy (i.e., RegCM) is designed to investigate those climate conditions over the various CORDEX-CORE and its sub-regions across the globe. Simulation of extreme events using RegCM will be helpful to understand the capability of the model for providing sufficiently advanced intimation of the occurrence of the extreme events which eventually will be beneficial for the policy planning and management of the country.

Dash et al. (2015) have shown that the RegCM is successfully able to simulate the monsoon circulation over the Indian subcontinent. Furthermore, several successful attempts have taken to simulate the ISM intra-seasonal and inter-annual using different parameterization schemes (Bhatla et al. 2016, 2018, 2019; Ghosh et al. 2019; Shahi et al. 2021). Several scientists (Sinha et al. 2013; Maharana and Dimri 2016; Bhatla et al. 2016; Ghosh et al. 2019; Verma and Bhatla 2021) show the importance of the parameterization scheme in simulating the characteristics of ISM. Hence, the choice of a suitable parametrization scheme is very important while dealing with the RegCM simulation for a specific purpose (Pal et al. 2007; Bhatla et al. 2016). The performance of RegCM can be improved using the concept of mixed parameterization as suggested by Giorgi et al. (2012) and further the mixed CPS shown satisfactory performance in simulating the ISM variability (Ali et al. 2015; Maity et al. 2017; Ghosh et al. 2019; Sinha et al. 2019; Verma and Bhatla 2020; Verma et al. 2021; Shahi et al. 2021). Furthermore, it is seen that the appropriate adjustment of moisture flux in the RegCM can significantly improve the precipitation distribution and intensity (Mohanty et al. 2019). An attempt in simulating rainfall and temperature using RegCM4.3 is performed over the southeast Asia CORDEX domain and found that the RegCM is able to simulate the climate extremes using Emanuel scheme over a complex topography (Ngo-Duc et al. 2017). In recent times, various modifications and up-gradations are going on to increase the RegCM efficacy. Therefore, another contribution has been attempted in this present study to support the ICTP RegCM community to utilize the model in simulating and projecting the extreme rainfall events at a regional/local scale with an aim to investigate the downscaling capabilities of RegCM. An endeavour has been made to utilise the version RegCM4.6 to successfully capture the extreme rainfall event over a complex topography, such as India. The case study has been chosen for the extreme event over Mumbai on July 26th, 2005 and the investigation is associated with synoptic, dynamic, and thermodynamic aspects.

2 Model description and methodology

The RegCM4.6 is developed at ICTP, Italy to utilise the model simulation for climate study. The ECMWF Interim Reanalysis (EIN15) data (Simmons et al. 2007) at $1.5° \times 1.5°$ horizontal grid resolution with 37 vertical levels and National Oceanic and Atmospheric Administration (NOAA)'s weekly optimal interpolation (OI_WK) sea surface temperature (OISST) data sets at $1° \times 1°$ resolution (Reynolds et al. 2007) are used as an initial and boundary condition. A brief on the model hydrostatic of RegCM4.6 is provided in Table 1 and the model physics can be obtained from Giorgi et al. (2012). There are four core CPSs available in RegCM4.6 viz. Kuo (Anthes et al. 1987), Grell (1993), Emanuel (1991), and Tiedtke (1989). While other than these four schemes, RegCM4.6 is capable to run the model simulation with a combination of two CPSs among them by choosing one scheme over land and another one over the ocean. In the present study, three core CPSs, namely, Grell, Emanuel, and Tiedtke, are considered along with their six different combinations, i.e., 1. Grell over land and Tiedtke over the ocean (GL_TO), 2. Tiedtke over land and Grell over the ocean (TL_GO), 3. Grell over land and Emanuel over the ocean (GL_EO), 4. Emanuel over land and Grell over ocean (EL_GO), 5. Emanuel over land and Tiedtke over the ocean (EL_TO) and 6. Tiedtke over land and Emanuel over the ocean (TL_EO) (Table 1). For the study requirement, the model is set up with the hydrostatic dynamical core over the SA-CORDEX domain (22°S–50°N and 10°E–130°E) from July 1st, 2005 to July 30th, 2005 with a horizontal resolution of 25 km and sigma vertical level of 18 for 6 h' time step. To avoid the noise, initial 20 days from the simulation period is considered as the spin-up time. The model simulated rainfall, mean sea level pressure (MSLP), wind (U and V components), relative and specific humidity, and pressure vertical velocity have been considered for the current

Table 1 Detailed description of RegCM4.6

Regional climate model (RegCM4.6)	
Model dynamics	Hydrostatic
Horizontal and vertical resolution	25 km with 18 vertical sigma levels
Initial and boundary conditions	ECMWF ERA Interim reanalysis (EIN15)
Sea surface temperature (SST)	OI_WK-OISST weekly optimal interpolation data set
Radiation scheme	NCAR CCM3 (Community Climate Model 3; Kiehlet al.1996)
Land surface model	Biosphere–Atmosphere Scheme (BATS) (Dickinson et al. 1989)
Planetary boundary layer scheme (PBL)	Holtslag (Holtslaget al. 1990)
Large-scale precipitation scheme	Subgrid Explicit Moisture Scheme (SUBEX), Sundqvist et al. 1989
Convective parametrization schemes	1.Grell 2.Emanuel 3.Tiedtke 4.Emanuel over land; Grell over ocean (EL_GO) 5.Grell over land; Emanuel over ocean (GL_EO) 6.Grell over land; Tiedtke over ocean (GL_TO) 7.Tiedtke over land; Grell over ocean (TL_GO) 8.Emanuel over land; Tiedtke over ocean (EL_TO) 9.Tiedtke over land; Emanuel over ocean (TL_EO)

study. Furthermore, model simulated rainfall is compared with the driving EIN15 reanalysis rainfall at 1.5° × 1.5° horizontal resolution and 3-h Tropical Rainfall Measurement Mission (TRMM) data set with the horizontal resolution of 0.25° × 0.25°for rainfall (Adler et al. 2000; Huffman et al. 2007). EIN15 6 h's data with the horizontal resolution of 1.5° × 1.5°is used for verification of the model simulated wind. The RegCM4.6 simulated relative and specific humidity, MSLP, and pressure vertical velocity are re-gridded to 2.5° × 2.5° horizontal resolution to validate the model performance with NCEP reanalysis.

Spatial distribution of accumulated rainfall over Mumbai and its adjoining areas has been analysed over the Santacruz rain gauge station for the period of July 25th to July 27th. To evaluate the model performance, each CPS is assessed using Taylor's diagram (Taylor 2001) with TRMM rainfall data over Santacruz. Taylor's diagram assesses similarity between the observed and model simulated fields by evaluating the correlation coefficient (CC), root-mean-square error (RMSE), and standard deviation (SD). Furthermore, these parameters are represented by a single dot on a two-dimensional plot. The statistical method is applied in this process to evaluate whether the performance of model simulation is in accordance with the observation or not. The model data, which is in good fit with the observation, must have high CC, low RMSE, and significant SD with their position nearer to the observational point. Mathematically, the formula of Taylor's diagram is:

$$E'^2 = \sigma_f^2 + \sigma_r^2 + 2\sigma_f\sigma_r\rho$$

where ρ is the CC between model and observation, E' is the RMS difference between model and observation, where σ_f^2 and σ_r^2 are the variances of the model simulation and observation, respectively.

The MSLP, wind pattern, relative humidity and the pressure vertical velocity at vertical atmospheric levels viz. 850 hPa and 500 hPa have been analysed. The association of the thermodynamical and dynamical aspects are investigated with the help of Hovmoller diagrams and time height cross section of various model simulated parameters, such as pressure vertical velocity, relative humidity, mass fraction of cloud liquid water etc.

3 Results and analysis

3.1 Spatial distribution of rainfall pattern

The spatial distribution of accumulated rainfall on July 26th, 2005 simulated using different CPSs of RegCM4.6 along with TRMM and EIN15 rainfall distribution are illustrated in Fig. 1. Figure 1a shows the TRMM rainfall, Fig. 1c–k shows the model simulated rainfall using different CPSs and Fig. 1b depicts the EIN15 reanalysis rainfall distribution over the area of interest. The observed accumulated rainfall for the period of 24 h has shown a maximum of 350 mm on the respective day of Mumbai extreme, while the rainfall distribution is ranging from 10 to 290 mm over the adjoining parts. The rainfall near Mumbai coastal areas is gauged around 130 mm, where a 50 mm of rainfall has been depicted over the Arabian Sea. The model simulated rainfall shows 10 mm to 450 mm rainfall distribution in nine different CPSs. Grell CPS simulates around 210 mm of rainfall (Fig. 1c) on that day which is less than the observed pattern, while it overestimates the rainfall in some of the adjoining

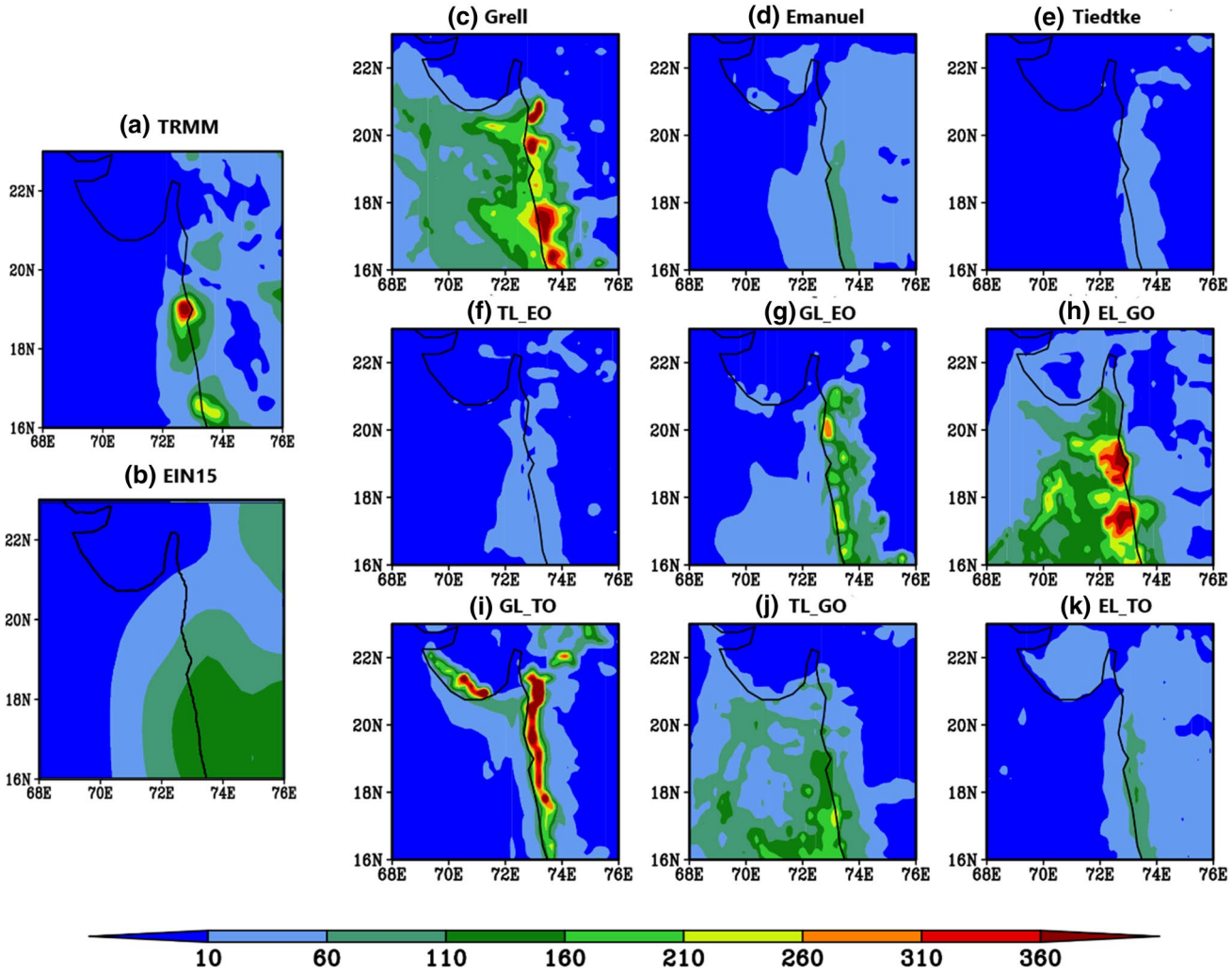

Fig. 1 Spatial distribution of accumulated daily rainfall (mm) obtained from observations (TRMM) and RegCM model simulations with different cumulus schemes for 26th July 2005 (16°–23°N and 68°–76°E)

areas of the western Indian peninsula (Surat and Western Ghat). The Grell CPS also overestimates the rainfall distribution over the Arabian Sea as compared with the observed rainfall data. CPS Emanuel simulated rainfall over Mumbai has shown a maximum value of 90 mm (Fig. 1d). Though, the rainfall amount in Emanuel CPS is very less than the observed rainfall, but unlike the CPS Grell, Emanuel shows a uniform band of rainfall distribution (90 mm) over the southern adjoining areas of Mumbai. CPS Tiedtke underestimates the rainfall amount (range between 10 and 50 mm) over Mumbai and the nearby areas along with a good rainfall estimation over the sea region (Fig. 1e). In Fig. 1f, the mixed CPS TL_EO shows similar result as of Tiedtke over land because of the mixing with the same CPS over land, and the oceanic part follows the rainfall distribution of Emanuel, as the Emanuel CPS is forced over the ocean. The GL_EO mixed CPS shows a good agreement with the observation (Fig. 1g) than TL_EO, Emanuel and Tiedtke. It is also observed that the GL_EO is able to simulate the rainfall distribution within the range of 10–330 mm over Mumbai and its surrounding areas but with a northward shift in the heavy rainfall location. The performance of the EL_GO CPS also shows a good agreement with observation and simulates the rainfall amount up to 400 mm over Mumbai and an overestimation is observed near 17°N,73.5°E compared (Fig. 1h) with TRMM rainfall. The simulation of EL_GO CPS over the Arabian Sea is quite similar to the Grell CPS, though the performance is not up to the mark (shows overestimation) as compared with TRMM rainfall. Furthermore, simulation with the CPS EL_GO, it is observed that the spatial distribution of rainfall is ranging from 10 to 400 mm over the Arabian Sea, while most of the part of the Arabian Sea receives up to 60 mm rainfall in the observed rainfall except the coastal regions of Mumbai, where the amount is

in the range of 90–410 mm. CPS GL_TO is overestimating rainfall by simulating up to 500 mm of rainfall over Mumbai and, the southern and northern regions of Maharashtra (Fig. 1i). The model simulated all CPSs are performed very similar over the Arabian Sea, except the Grell and those mixed CPSs whose oceanic section is mixed with the Grell CPS. Mixed CPS TL_GO shows less amount of accumulated rainfall over Mumbai (170–210 mm) (Fig. 1j) when compared with the TRMM rainfall and the performance of this CPS is fairly good over the coastal areas of Mumbai. The spatial distribution of rainfall using EL_TO finds a band of 50–130 mm rainfall over Mumbai and the surrounded region of 16°–20.8°N and 73.8°E (Fig. 1k). Most of the considered CPSs, namely, Grell, GL_EO, EL_GO, GL_TO, and TL_GO, have satisfactorily simulated the rainfall (close to the observation) when compared to the driving EIN15 which shows only 60–100 mm of rainfall distribution over the region of interest (Fig. 1b). Furthermore, RegCM4.6 with CPSs Grell, EL_GO and GL_TO have downscaled the reanalysis EIN15 data with better accuracy in spatio-temporal aspects. Based on the above discussion it can be stated that the Grell CPS has performed very well over the ocean section either as a core CPS or in mixed CPS mode.

3.2 Time series analysis of 6 hourly accumulated rainfall at Santacruz in Mumbai

The 6-h accumulated rainfall time series for three consecutive days viz. 25th, 26th, and 27th July over Santacruz rain gauge station (19.09°N, 72.85°E) is shown in Fig. 2. The accumulated TRMM rainfall illustrates that the maximum rainfall of ~ 145 mm is occurred around 12 UTC (26th July) which is gradually decreased by 18 UTC on 27th July. It is found that the Tiedtke, TL_EO, and EL_TO CPSs have poorly captured the event with a maximum amount of ~ 20 mm rainfall throughout the period. However, the Emanuel, GL_EO, GL_TO, and TL_GO CPSs have shown some improvements with a maximum rainfall in the range of 20–60 mm. Whereas, the performance of Grell CPS is satisfactory (maximum rainfall > 160 mm); however, it shows the maximum rainfall in prior to the actual time of heavy rainfall episode during 18UTC on 25th July. The maximum rainfall of ~ 140 mm at 12 UTC on 26th July is well simulated by the mixed CPS EL_GO, while a sudden decrease in rainfall has been noticed around 18 UTC on 26th July which is not in accordance with the actual rainfall event. However, the performance of mixed CPS EL_GO has shown a closer pattern as observed and simulated nearly 113 mm of rainfall, where the TRMM shows ~ 93 mm of rainfall accumulation during 00 UTC on 27th July. TRMM rainfall shows ~ 345 mm of accumulated rainfall, while the model has simulated ~ 389 mm of rainfall using EL_GO CPS on 26–27th July (within 24 h) which is quite interesting. On the other hand, reanalysis EIN15 have shown ~ 35 mm of rainfall around 12 UTC (when the maximum rainfall of ~ 345 mm is observed) along with 110 mm of accumulated rainfall within 24 h. Most of the CPSs have shown significantly better results when compared with the EIN15 reanalysis which highlights the capability of RegCM4.6 in reproducing the temporal distribution of rainfall as well as intensity. To evaluate the performance of RegCM4.6 in present study Taylor's diagram has been used (Fig. 3). In Fig. 3a, forcing EIN15 data has been considered as reference to investigate the performance of RegCM4.6. From figure, it can be seen that the Grell, Tiedtke, GL_TO, and TL_GO are having nearly 0.2, 0.1, 0.15 and 0.2 CC values, respectively along with more than 1 RMSE values. Similarly, Fig. 3b represents Taylor's diagram with various CPSs, where the TRMM rainfall

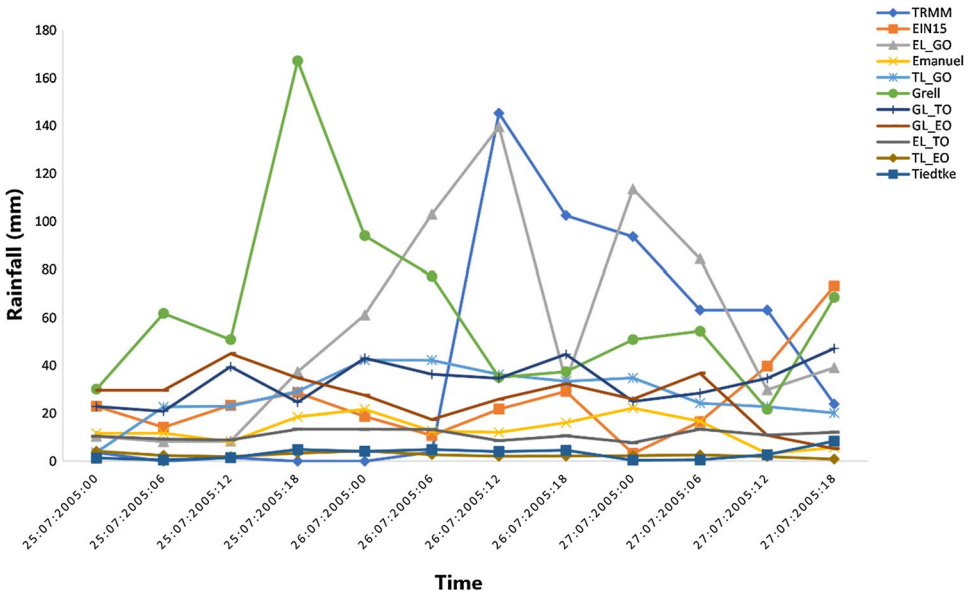

Fig. 2 Time series of 6-h rainfall (mm) accumulations over Santacruz (19.09°N,72.85°E) in Mumbai during the period 25th July to 27th July 2005 shown for observations an RegCM simulations with various CPSs

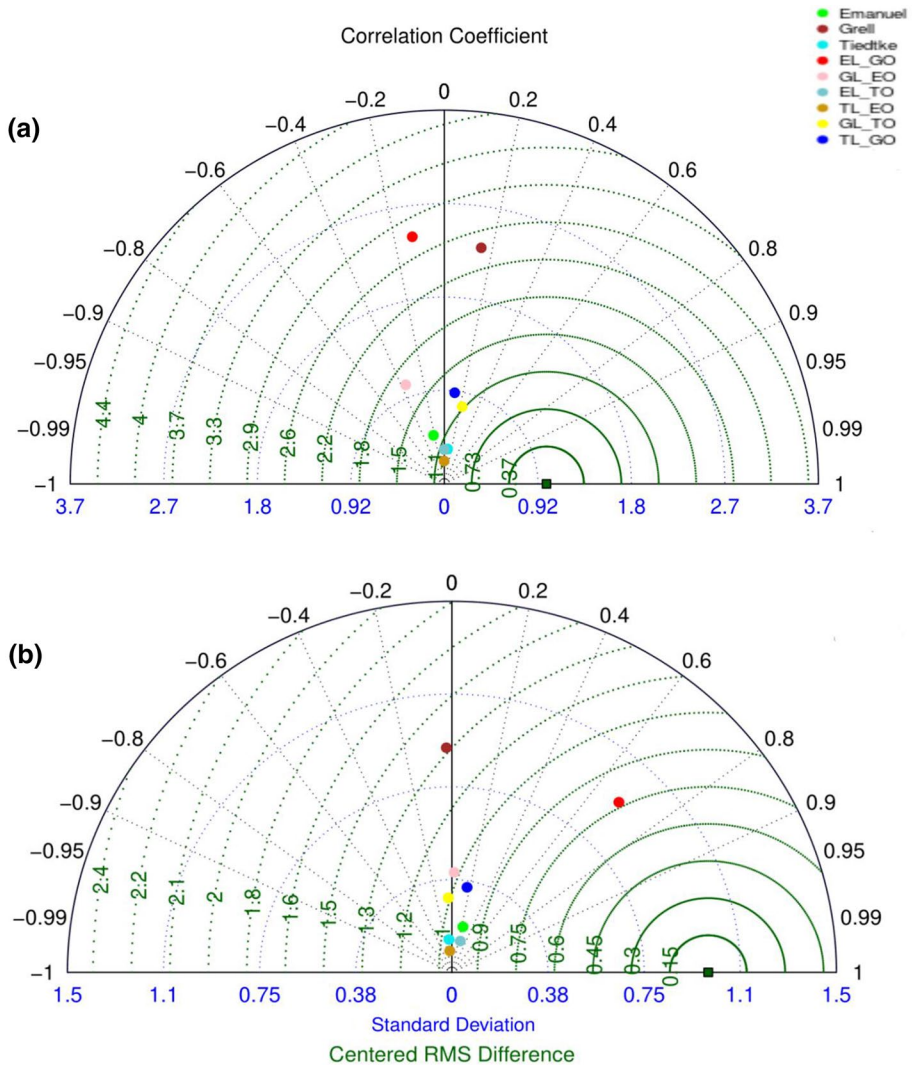

Fig. 3 Taylor's diagram for **a** EIN15 and **b** TRMM rainfall vs model simulated rainfall with various CPSs over Santacruz, Mumbai

data has been chosen as reference. Figure suggests that the mixed CPSs, namely, EL_GO, Emanuel, TL_GO, EL_TO, and GL_EO, have shown positive CC (> 0.2), whereas the rest of CPSs viz. Grell, Tiedtke, TL_EO, and GL_TO are having very small (< 0.1) CC values with TRMM rainfall. It can be seen that the mixed CPS EL_GO shows much better CC (~ 0.7) among all the considered CPSs. As far as the SD is considered all the CPSs except EL_GO and EL_TO have shown values in the range 0 to 0.38 mm which is very far as compared to the TRMM rainfall, while EL_GO and Grell CPSs depicts values ~ 1 mm. Furthermore, the CPS EL_GO shows least RMSE as compared to the other CPSs. Therefore, the mixed CPS EL_GO can be considered as best performing scheme due to its higher CC, less RMSE, and SD values close to the TRMM. A comparison of Fig. 3a, b suggests that the model simulated results are much closure to the high-resolution satellite TRMM data (0.25° × 0.25°) than the coarse resolution driving EIN15 (1.5° × 1.5°) due to the fact that Global Models are not able to capture the localized phenomena due to their coarser resolution. However, by dynamical downscaling of EIN15 to finer resolution using the regional climate model RegCM4.6, it can be seen that model has fairly simulated the localized heavy rainfall over Mumbai and results are in accordance with the observations. Moreover, the RegCM4.6 could able to bring out rainfall distribution and intensity better than its driving force when compared to the observations. Overall, analysis suggests that the RegCM4.6 with CPS EL_GO have performed well among all the nine CPSs considered in the present study.

3.3 Analysis of mean sea level pressure, relative humidity and pressure vertical velocity with wind

The daily MSLP of reanalysis and EL_GO CPS over the region 0°–35°N and 50°–95°E during the period 24–28th July 2005 is shown in Fig. 4. The left column (Fig. 4a) represents the formation of a low-pressure system (~ 1000 hPa)

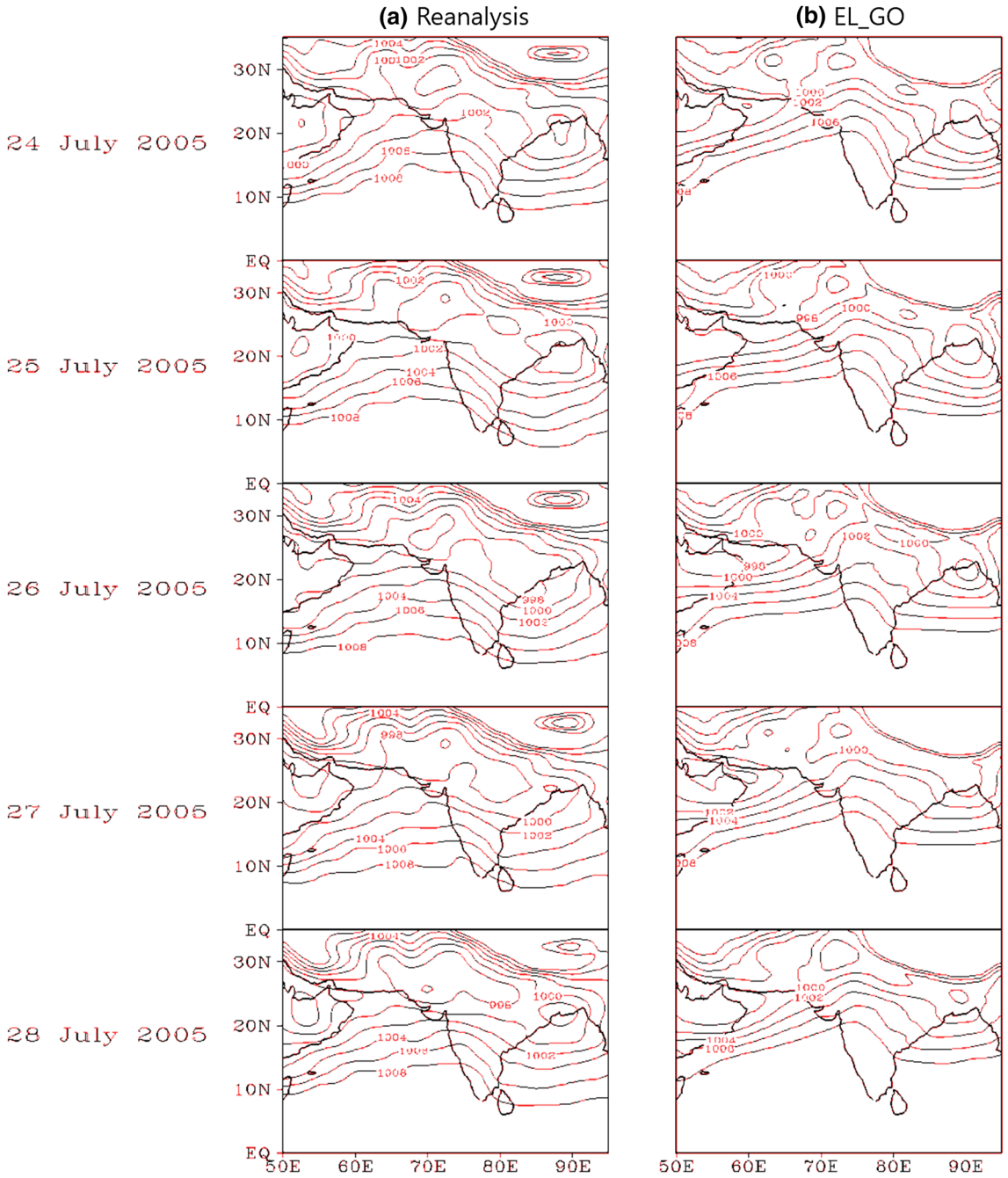

Fig. 4 Mean Sea Level Pressure (MSLP; in hPa) pattern for **a** NCEP reanalysis (left column) and **b** mixed CPS EL_GO (right column) over the region (0°–35°N and 50°–95°E) during 24th–28th July 2005

that has been started on 25th of July near the East coast, Orissa and BOB. A constant decrease pattern in MSLP is continued over the eastern coastal regions and BOB. It further becomes remarkable at 998 hPa on 26th July affecting the flow of moisture laden south-westerly monsoonal winds. The CPS EL_GO (Fig. 4b) has simulated the formation of the low-pressure system reasonably well. The condition of low-pressure system persists for up to 2 days, i.e., 26th and 27th July 2005. Such low-pressure system formed over the BOB often leads to a extremely heavy rainfall (more than 300 mm/day) over India and the southwestern region (Ajayamohan et al. 2010; Krishnamurthy and Ajayamohan 2010).

A comparison of reanalysis andEL_GO CPS wind (U and V) pattern along with the variation of relative humidity over the region 0°–30°N and 50°–95°E are shown in Fig. 5. Figure illustres that the 6-h variations in wind and the spatial

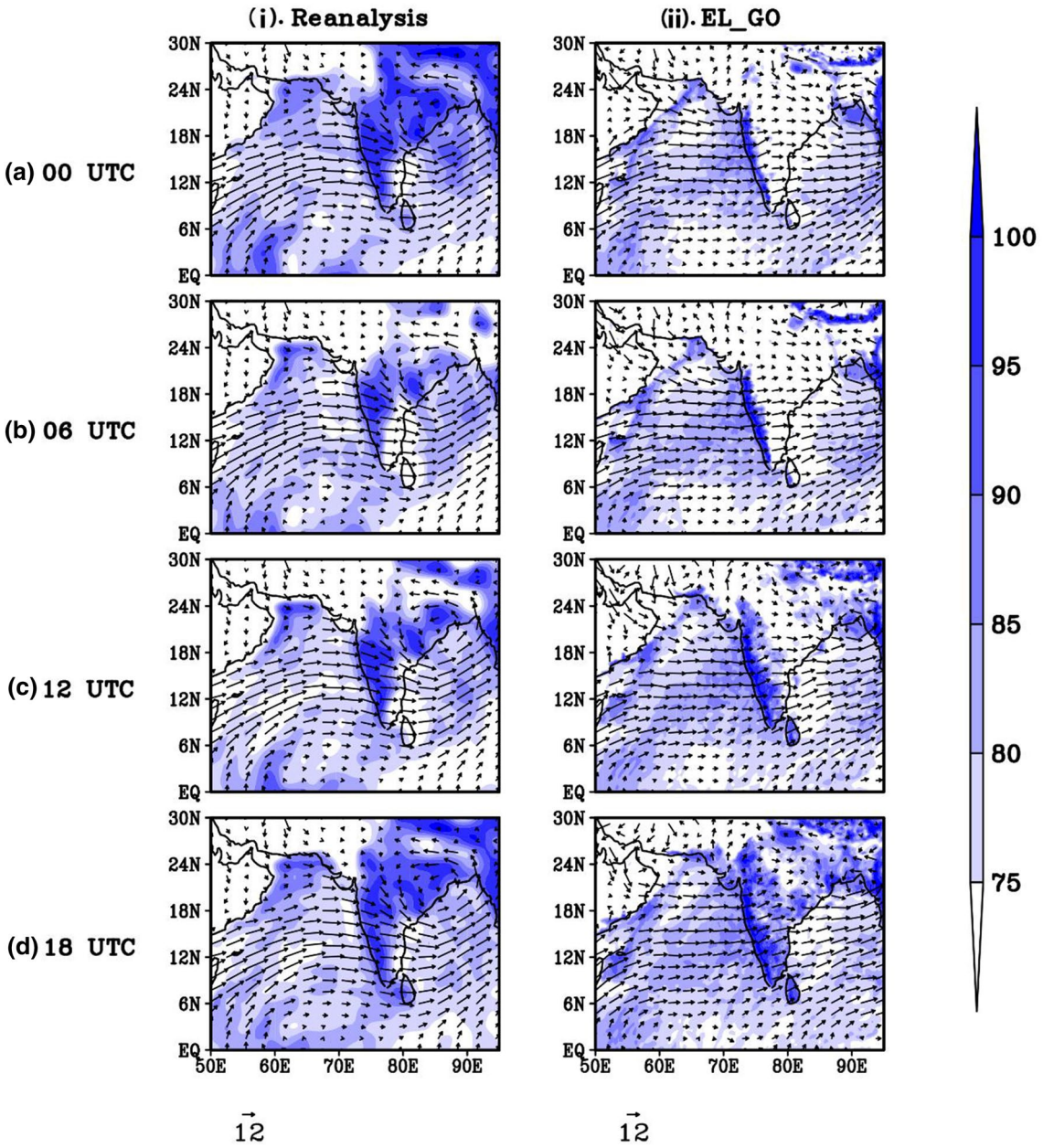

Fig. 5 Relative humidity (shaded; in %) and U–V Wind (vector; in m/s) at 850 hPa obtained fromi). reanalysis NCEP data and EIN 15, respectively (left column), and same figure for ii). mixed CPS EL_GO (right column) over the region (0°–30°N and 50°–95°E) during 26th July 2005

distribution of relative humidity at 850 hPa on 26th July 2005. Figure also confirms the genesis and development of the low-pressure system (cyclonic circulation) near Orissa and over north–west BOB (~ 20°N) at 00 UTC, where the reconcilement of low-level southwesterly and easterly winds takes place (Fig. 5i). The formation of this cyclonic circulation enhances the speed of moisture load through the southwesterly winds over Mumbai and Western Ghat regions and causes extremely heavy rainfall to occur over Mumbai. The presence of this cyclonic circulation over Orissa and BOB is well simulated by the model and can be seen in the right column (Fig. 5ii). Though, there is a slight shift to the right to its actual position. At the same time, the winds circulation are very intense (> 12 m/s) over Mumbai and Western Ghats. The relative humidity is well simulated by the model over Mumbai and its adjacent areas but its performance is not satisfactory over central and the northeast Indian regions. A band of 90–100% relative humidity can be noticed over Mumbai and adjacent areas including Western Ghats with the low-pressure system over BOB during the whole day from 00 to 18 UTC on the date of extreme event.

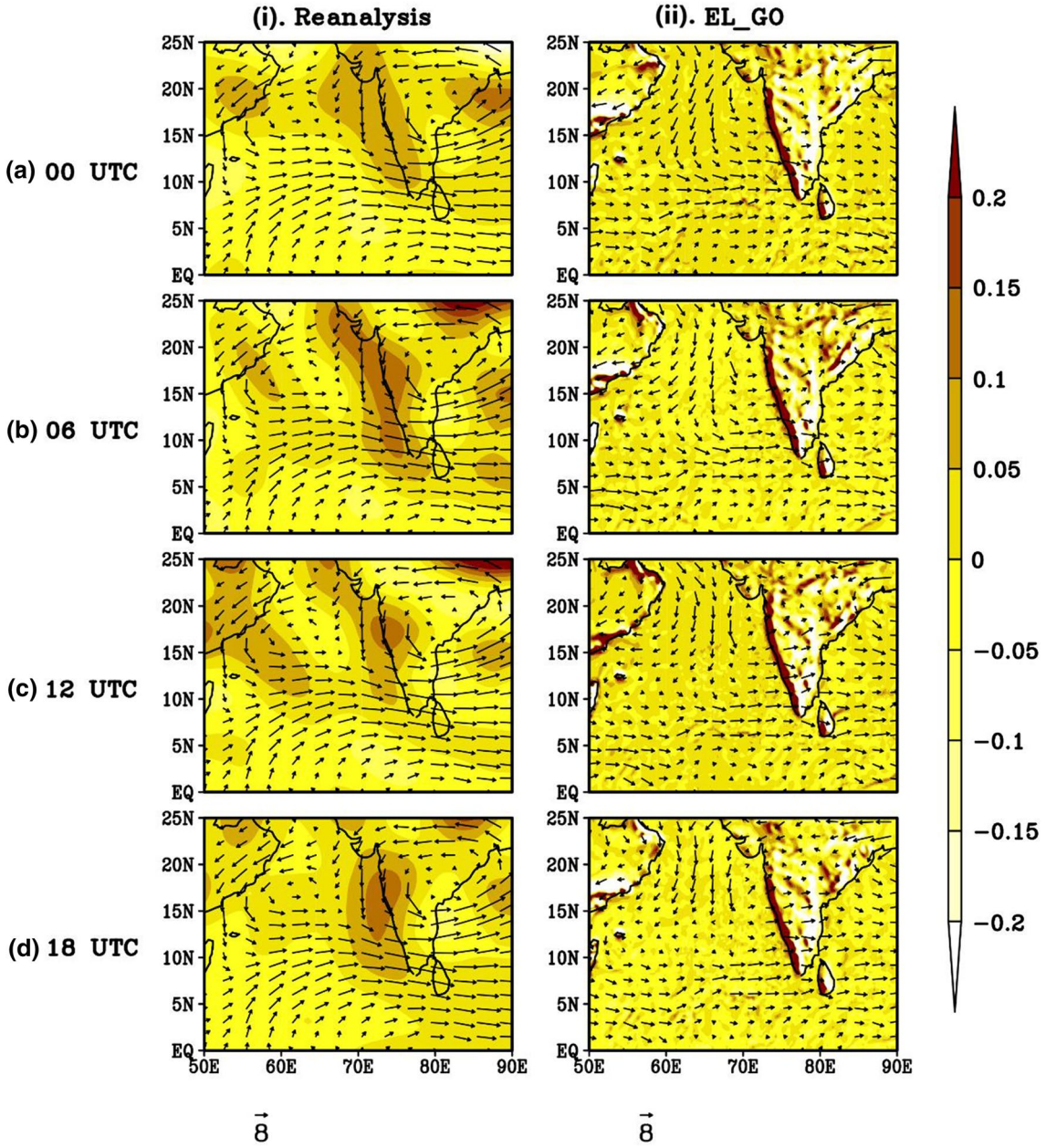

Fig. 6 Same as Fig. 5 but shown for pressure vertical velocity (in shaded and positive for upward motion;in Pa/s) and U–V Wind (vector;in m/s) at 500 hPa pressure level

A significant enhancement in the relative humidity can be noticed towards central India during 12 to 18 UTC.

The comparison of 6-h wind (U and V) and vertical pressure velocity at 500 hPa over the region 0°–25°N and 50°–90°E during 26th July is shown in Fig. 6. From the figure, a cyclonic structure due to a low-pressure system can be noticed using the reanalysis data with an enhanced proportion towards central India and western coastal regions (Fig. 6i). This pattern persists during the whole day with an intense wind with a magnitude of more than 8 m/s. A cyclonic circulation is formed over Mumbai and its nearby regions which is the conformation of MTC and can be a possible cause behind the extreme rainfall event (Kumar et al. 2008). These extremely heavy rainfall events are generally associated with MTC, off-shore troughs and vortices (Francis and Gadgil 2006; Pradhan et al. 2015). The observation pattern of the cyclonic circulation is also satisfactorily captured by the model during the same period with comparatively lower wind speed (Fig. 6ii). A same kind of low-pressure system can also be seen near 15°–22°N and 55°–62°E in both observed and model simulation. The positive pressure vertical velocity for upward motion shows a

continuous band of ~ + 0.1 Pa/s over the region 10°–25°N and 70°–76°E during 00 UTC on 26th July, whichis well simulated by the model but with a narrower continuous bands of higher values (> + 0.2 Pa/s). Furthermore, positive values over the Eastern coastal regions (near Orissa) and 20°N–55°E (western region) have been noticed which can also be seen in model simulated results, elsewhere the pressure vertical velocity is negative (shows a downward motion). The observation pattern shows that the intensity of pressure vertical velocity band got enhanced (+ 0.15 Pa/s) over Mumbai and the nearby regions and model still shows a higher value during 06 UTC. The band with pressure vertical velocity ~ + 0.15 Pa/s is still consistant but it has been enhanced up to + 0.2 Pa/s or more over Mumbai around 12 UTC. The model has satisfactorily simulated the same mechnanism but with a greater magnitude (more than + 0.2 Pa/s). The condition of higher pressure vertical velocity over Mumbai and adjoining area is persisted up to 18 UTC and the model shows its capacity to represent the similar pattern as it has shown during 12 UTC. The increased positive values of pressure vertical velocity over Mumbai and nearby regions prior to the extreme event may be the cause behind the supply of enormous amount of moisture from surface to the higher level which supports the occurrence of extremely heavy rainfall over Mumbai on 26th July, 2005.

3.4 Analysis of horizontal divergence

The horizontal divergence at the lower (850 hPa) and upper (200 hPa) levels over the region 17°–22°N and 71°–76°E during 06 and 12 UTC on 26th July has been presented in Fig. 7. A strong divergence of 2×10^{-5} to 4×10^{-5}/s is noticed at 06 UTC at 850 hPa (Fig. 7a), while at the same time a strong convergence or a negative divergence of -6×10^{-5} to -4×10^{-5}/s is noticed over 17°–19°N and 73°–73.5°E at 200 hPa (Fig. 7c). A confluence of divergence and convergence with small value can be seen over Mumbai and its surrounding areas at both of the levels (850 hPa and 200 hPa) during 06 UTC. At 12 UTC, a strong convergence of -6×10^{-5}/s (or less) at the lower level is accompanied by a strong divergence of 4×10^{-5}/s (or more) at the upper level is depicted during the heavy precipitation over Mumbai (especially near 19.09°N–72.85°E) (Fig. 7b–d). Some patches of lower level convergence and upper level divergence can also be seen at the northward and southward directions from the region of interest. This situation of lower level convergence and upper level divergence causes net upward motion which can be seen in Fig. 6c. Such features provide necessary conditions which are favourable for the formation of mesoscale system and severe convective activity that may lead to the heavy rainfall event to be occured (Goswami et al. 2013).

3.5 Analysis of latitudinal and longitudinal variation of wind with specific humidity (Hovmoller diagrams)

The Hovmoller diagram of EL_GO simulated 6-h wind (zonal and meridional) (unit in m/s) superimposed with the specific humidity (g/kg) at 850 hPa along with the rainfall (mm) during the period 25th–27th July is shown in Fig. 8. The latitudinal variation of zonal (u) wind with specific humidity superimposed (Fig. 8a) and rainfall (Fig. 8b) is considered between 3° and 30°N centred at 72.85°E. A significant amount of moisture (13.2 g/kg) with intense westerly wind (12 m/s or more) can be seen at 12°–15°N which is further extended towards the lower latitude during 00 UTC to 12 UTC on 25th July. A significant amount of rainfall between 80 and 100 mm can be found over the same region at the same time. The presence of very high specific humidity (13.6–14 g/kg or more) with higher wind velocities (westerlies) ranging from 8 to 14 m/s can be noticed over 14°–25°N during 00 to 12 UTC on 26th July. A closure investigation reveals that the maximum specific humidity (~ 14 g/kg) and westerly wind speed (~ 12 m/s or more) are present between 17° and 20°N from 12 UTC on 26th July to 06 UTC on 27th July which manifests the maximum rainfall (up to 140 mm) over the same location and time period and decreases later on (~ 40–80 mm) after 12 UTC on 27th July. The persistence of intense westerly (south westerlies during ISM period) wind could be the reason behind the enormous supply of moisture over these latitudes. The results are also in agreement with the TRMM rainfall (Fig. 2) over the location of heavy rainfall, i.e., over Santacruz (19.02°N, 72.85°E) in Mumbai.

The longitudinal variation between 60° and 90°E and centred at 19.09°N for meridional wind with superimposed specific humidity along with the rainfall distribution are shown in Fig. 8c, d. From Fig. 8c, it is observed that a plenty of moisture is present as the value of specific humidity showed bands is between 11 g/kg and 13 g/kg over 66°–72°E during the time 00 to 18 UTC on 25th July. However, the meridional wind (either towards the south or north) is not so intense during the whole scenario. A rainfall band of ~ 80 mm (Fig. 8d) at the same time and location seems to be following the evolution of specific humidity. The band of higher specific humidity gets enhanced (~ 14 g/kg and more) in between 71° and 75°E at 00 UTC during 26th July to 18 UTC on 27th July. A close observation in Fig. 8d depicts that the highest rainfall (140 mm or more) has been occurred near 71°–73°E after 00 UTC on 26th July to 18 UTC on 27th July. However, a decrease in rainfall (~ 40 mm) is seen during 18 UTC on 26th July. As far as the meridional (v) wind component is concerned, the directions are southward during most of the time, where wind speed is very less with magnitude of 2 m/s excepts during 11 UTC and 18 UTC on 26th July

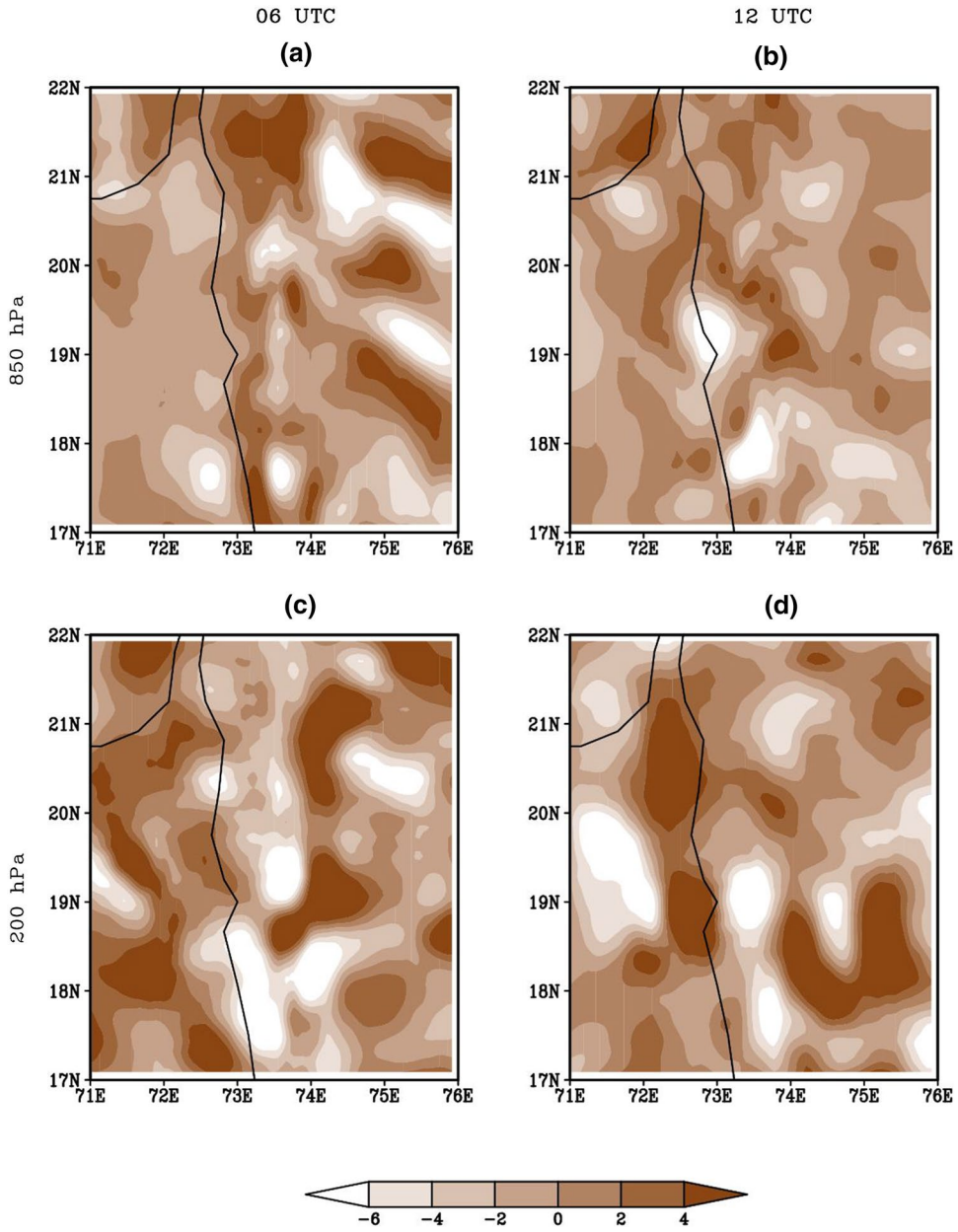

Fig. 7 Horizontal divergence ($\times 10^{-5}$/s) during the 06 UTC (Fig. **a, c**) and 12 UTC (Fig. **b, d**) of 26th July 2005 at lower level (850 hPa) and upper level (200 hPa) for the mixed CPS EL_GO over the region (17°–22°N and 71°E–76°E)

over the 63°–71°E (left to the place of heavy rainfall). The whole mechanism supports the favourable conditions for an extreme heavy rainfall event that was occurred on 26th July 2005 over Mumbai.

3.6 Analysis of vertical structure and involved thermodynamics at the location of heavy rainfall event

The thermodynamic and dynamic aspects provide the favourable genesis conditions to an extreme rainfall event and affect with several processes during its different stages (Pfahlet al. 2017; O'Gorman 2015). To investigate such aspects, the model simulated rainfall features related to the vertical structure of atmosphere has been discussed over the location of heavy precipitation (Santacruz rain gauge station at 19.09°N and 72.85°E) during 25–27th July 2005 (Fig. 9). Figure 9a shows the time height cross section of divergence and it can be demonstratedfrom the figure that the convergence (negative divergence) is exhibited at mid-tropospheric level (around 500 hPA) and 800 hPa prior to the 00 UTC on 26th July and during the maximum rainfall (around 12 UTC on 26th July) (Fig. 9d) which persists during 00 UTC on 27th July. A strong divergence of 3.5×10^{-5}/s can be noticed over the mid-lower troposphere (near 700hPA) during the considered time which makes a contrasting feature with lower levels (near the surface) and mid troposphere. A closure look reveals that at the upper levels (250–200 hPa), a

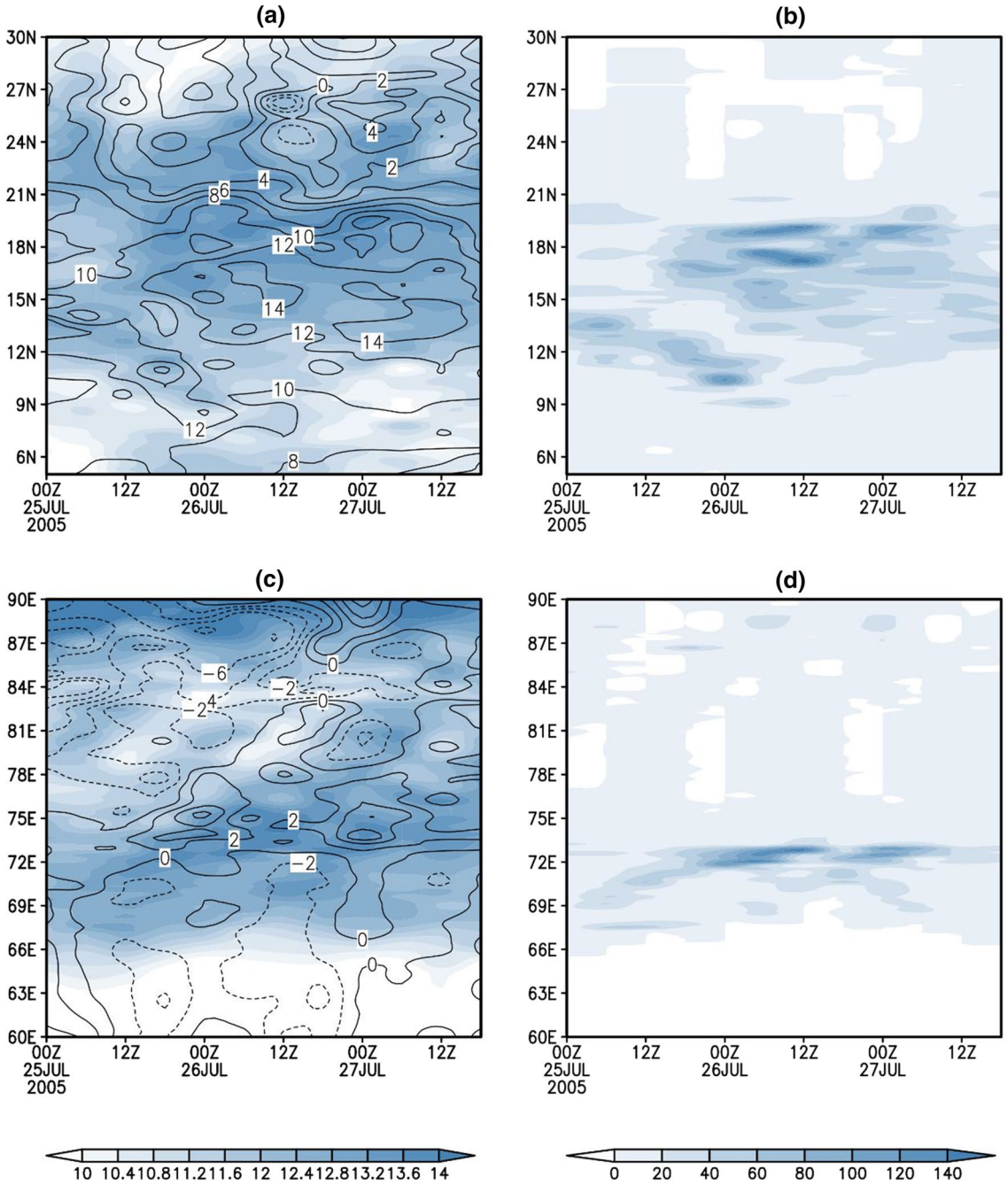

Fig. 8 Hovmoller diagram computed for the wind and specific humidity in zonal and meriodional direction over Santacruz (19.09°N, 72.85°E) location. **a** U-wind speed (contour; in m/s) and specific humidity (shaded; in g/kg) at 850 hPa in zonal direction, **b** Rainfall (in mm) distribution over 3°N–30°N and 72.85°E, **c** same as (**a**) but for V-wind speed (contour; in m/s) and specific humidity (shaded) in meridional direction, and **d** Rainfall (in mm)distribution over 19.09°N and 60°E–90°E during the period 25th–27th July 2005

strong divergence is present along with a strong convergence at lower levels near to the surface (1000–800 hPa) before and during the heavy rainfall (Vaidya and Kulkarni 2008). Two maxima in rainfall first up to 140 mm of rainfall at 12 UTC on 26th July and another one just before 00 UTC on 27th July (~ 118 mm) are noticed in Fig. 9d which are accompanied with the lower level convergence and upper level divergence structure that enhances the convective activities during the event (Goshwami et al. 2013).

The situation of lower level convergence and upper level divergence prompt the net upward motion which is supported by the pressure vertical velocity (values are positive for upward motion in Fig. 9b). It can be depicted that the vertical motions (pressure vertical velocity) are positive and

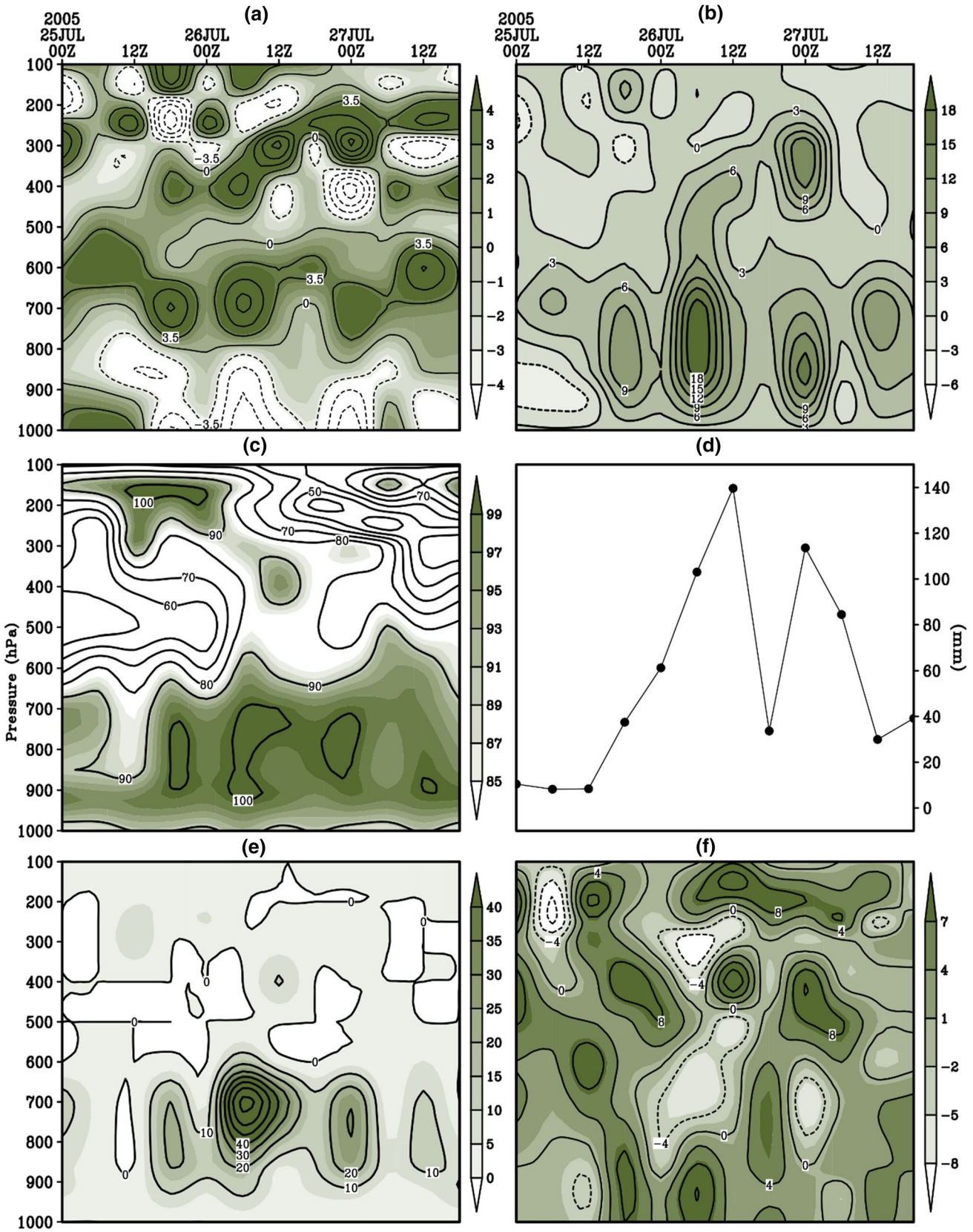

Fig. 9 The time height cross section **a** divergence ($\times 10^{-5}$/s), **b** pressure vertical velocity ($\times 10^{-3}$) hPa/s (positive for upward motions), **c** relative humidity (%), **d** 6-hour rainfall (mm), **e** mass fraction of cloud liquid water ($\times 10^{-2}$ g/Kg) and **f** vorticity ($\times 10^{-5}$/s), at location (19.09°N and 72.85°E) during 25th–27th July 2005

intense (6×10^{-3}–18×10^{-3} hPa/s) at the mid and lower levels (between 1000 and 450 hPa) during 00 UTC to 10 UTC on 26th July. The maximum vertical pressure velocity up to 18×10^{-3} hPa/s or more can be noticed in between the levels of 850–600 hPa. The presence of sufficient amount of moisture in the atmosphere is a necessary aspect for the occurrence of such an extremely heavy rainfall event in addition to the intense vertical motions. Figure 9c shows that a large amount of moisture (relative humidity) is present near the surface throughout the event which further extended up to the mid tropospheric level. A band of high relative humidity extending from surface to 600 hPa has also been noticed which is supported by the lower level convergence and intense vertical motions that causes the rainfall amount of ~ 60 mm during 18 UTC on 25th July. It is to be noticed that the maximum amount of moisture (relative humidity ~ 100%) is present over lower and mid troposphere prior to the extreme rainfall, i.e., before 12 UTC on 26th July. This situation can be explained in such a way that the strong convergence at lower level causes intense vertical motion and pumps a lot of moisture from lower to the near mid troposphere. It can also be confirmed by the presence of maximum mass fraction of cloud liquid water (20×10^{-2}–40×10^{-2} g/kg) as in Fig. 9e. The vertical motion get slow (Fig. 9b) and the amount of moisture in lower and mid troposphere become low (Fig. 9c) along with the disappearance of cloud liquid water fraction (Fig. 9e) after and during 12 UTC on 26th July, where the maximum rainfall takes place (Fig. 9d; Sahany et al. 2010). Another rise in rainfall (~ 118 mm) can be observed after 18 UTC on 26th July followed by a sudden drop of rainfall in between at 12 UTC and 18 UTC on the same day. This scenario can also be explained like: the presence of lower level convergence prompts intense vertical motion which pumps a plenty of moisture in lower and mid troposphere, and the formation of dense cloud (high mass fraction of cloud liquid water) takes place which and results of heavy rainfall. The higher values of positive/cyclonic vorticity (~ 7×10^{-5}/s) can be seen near the surface (extending towards lower tropospheric level) around 18 UTC on 25th July and before 12 UTC on 26th July (Fig. 9f). The positive vorticity at lower level supports the divergence in upper level and net upward vertical motion which favours the deep convection.

4 Summary and conclusions

The authors have tried to capture the rainfall extreme over Mumbai occurred on 26th July 2005 and, therefore, have considered the coarser resolution of forcing data of EIN15 with a resolution of $1.5°\times1.5°$ to producea high-resolution ($0.25°\times0.25°$) dynamical downscaled data using RegCM4.6. From the forcing rainfall data by EIN15, it is very hard to see the rainfall extreme over Mumbai which is clearly visible in the TRMM rainfall for the respective days. It may be due to the coarser resolution of EIN15 rainfall data. The RegCM4.6 performance has been evaluated with TRMM rainfall and it is found that the RegCM4.6 performs significantlywell when model is setup in mixed cumulus parameterization schemes mode. The spatio-temporal distribution of accumulated rainfall (within 24 h) shows that the Grell, GL_TO, and EL_GO CPSs have performed satisfactorily compared to the other CPSs. Furthermore, EL_GO shows the best performance by capturing the highest peak of extreme rainfall along with the region of heavy rainfall with significant accuracy on 26th July as compared toTRMM rainfall. By incorporating the dynamical downscale using RegCM4.6 with the coarse resolution data of EIN15, it is possible to capture the extreme rainfall events over the regional scale (e.g. Mumbai extreme rainfall events on 26th July 2005), and the effort of the regional climate modeler community get success and the concept of dynamical downscaling get another level of attention to study the regional/local scale phenomena.

Acknowledgements Authors wish to show their sincere gratitute to two anonymous reviewers who put their significant efforts through their valuable comments and suggestions to improve the quality of this work. This work is a part of a R&D project, funded by Department of Science and Technology (DST), Govt. of India in the form of Centre for Excellence in Climate Change. Thanks to the India Meteorology Department (IMD), NOAA/OAR/ESRL, NCEP, TRMM and ECMWF for providing the necessary gridded data sets. Special thanks to Abdus Salam International Center for Theoretical Physics (ICTP), Italy for providing RegCM4.6.

Data availability The data sets generated/analyzed during the current study are available from the corresponding author on reasonable request.

Declarations

Conflict of interest The authors declare that they have no conflict of interest.

References

Ajayamohan RS, Merryfield WJ, Kharin VV (2010) Increasing trend of synoptic activity and its relationship with extreme rain events over central India. J Clim 23(4):1004–1013

Adler RF, Huffman GJ, Bolvin DT, Curtis S, Nelkin EJ (2000) Tropical rainfall distributions determined using TRMM combined with other satellite and rain gauge information. J ApplMeteorol 39(12):2007–2023

Ali S, Dan L, Fu C, Yang Y (2015) Performance of convective parameterization schemes in Asia using RegCM: simulations in three typical regions for the period 1998–2002. Adv Atmos Sci 32(5):715–730

Almazroui M, Saeed S, Saeed F, Islam MN, Ismail M (2020) Projections of precipitation and temperature over the South Asian countries in CMIP6. Earth Syst Environ 4(2):297–320
Anthes RA, Hsie EY, Kuo YH (1987) Description of the Penn State/NCAR mesoscale model version 4 (MM4). NCAR Techni Note 282+STR
Ashfaq M (2020) Topographic controls on the distribution of summer monsoon precipitation over South Asia. Earth Syst Environ 4:667–683
Baisya H, Pattnaik S (2019) Orographic effect and multiscale interactions during an extreme rainfall event. Environ Res Commun 1(5):051002
Benson CL Jr, Rao GV (1987) Convective bands as structural components of an Arabian Sea convective cloud cluster. Mon Weather Rev 115(12):3013–3023
Bhatla R, Ghosh S, Mall RK, Sinha P, Sarkar A (2018) Regional climate model performance in simulating intra-seasonal and interannual variability of Indian summer monsoon. Pure Appl Geophys 175(10):3697–3718
Bhatla R, Ghosh S, Mandal B, Mall RK, Sharma K (2016) Simulation of Indian summer monsoon onset with different parameterization convection schemes of RegCM-4.3. Atmos Res 176:10–18
Bhatla R, Verma S, Ghosh S, Mall RK (2019) Performance of regional climate model in simulating Indian summer monsoon over Indian homogeneous region. Theor Appl Climatol 139:1121–1135
Bohra AK, Basu S, Rajagopal EN, Iyengar GR, Gupta MD, Ashrit R, Athiyaman B (2006) Heavy rainfall episode over Mumbai on 26 July 2005: Assessment of NWP guidance. Curr Sci 90(9):1188–1194
Das S, Ashrit R, Iyengar GR, Mohandas S, Gupta MD, George JP, Rajagopal EN, Dutta SK (2008) Skills of different mesoscale models over Indian region during monsoon season: forecast errors. J Earth Syst Sci 117(5):603–620
Das SK, Gupta RK, Varma HK (2007) Flood and drought management through water resources development in India. Bull World Meteorol Org 56(3):179–188
Dash SK, Pattnayak KC, Panda SK, Vaddi D, Mamgain A (2015) Impact of domain size on the simulation of Indian summer monsoon in RegCM4 using mixed convection scheme and driven by HadGEM2. Clim Dyn 44(3–4):961–975
Dhar ON, Nandargi S (1998) Rainfall magnitudes that have not been exceeded in India. Weather 53(5):145–151
Dickinson RE, Errico RM, Giorgi F, Bates GT (1989) A regional climate model for the western United States. Clim Change 15(3):383–422
Dodla VBR, Ratna SB (2010) Mesoscale characteristics and prediction of an unusual extreme heavy precipitation event over India using a high-resolution mesoscale model. Atmos Res 95(2–3):255–269
DST (2001) Arabian Sea monsoon experiment science Plan. New Delhi
Emanuel KA (1991) A scheme for representing cumulus convection in large-scale models. J Atmos Sci 48(21):2313–2329
Francis PA, Gadgil S (2006) Intense rainfall events over the west coast of India. Meteorol Atmos Phys 94(1–4):27–42
Ghosh S, Das D, Kao SC, Ganguly AR (2012) Lack of uniform trends but increasing spatial variability in observed Indian rainfall extremes. Nat Clim Change 2(2):86–91
Ghosh S, Bhatla R, Mall RK, Srivastava PK, Sahai AK (2019) Aspect of ECMWF downscaled Regional Climate Modeling in simulating Indian summer monsoon rainfall and dependencies on lateral boundary conditions. Theor Appl Climatol 135(3–4):1559–1581
Giorgi F et al (2012) RegCM4: model description and preliminary tests over multiple CORDEX domains. Clim Res 52:7–29
Goswami BN, Venugopal V, Sengupta D, Madhusoodanan MS, Xavier PK (2006) Increasing trend of extreme rain events over India in a warming environment. Science 314(5804):1442–1445
Goswami P, Himesh S, Goud BS (2013) Simulation of high-impact tropical weather events: comparative analysis of three heavy rainfall events. Nat Hazards 65(3):1703–1722
Grell GA (1993) Prognostic evaluation of assumptions used by cumulus parameterizations. Mon Weather Rev 121(3):764–787
Guhathakurta P, Sreejith OP, Menon PA (2011) Impact of climate change on extreme rainfall events and flood risk in India. J Earth Syst Sci 120(3):359
Gulf News (30th August 2018) Kerala flood live: Hundreds dead, hundreds of thousands homeless, clean-up drive starts| GulfNews.com. Retrieved from https://gulfnews.com/news/asia/india/kerala-flood-live-hundreds-dead-hundreds-of thousands-homeless-clean-up-drive-starts-1.226842
Huffman GJ et al (2007) The TRMM multisatellite precipitation analysis (TMPA): Quasi-global, multiyear, combined-sensor precipitation estimates at fine scales. J Hydrometeorol 8:38–55
Jenamani RK, Bhan SC, Kalsi SR (2006) Observational/forecasting aspects of the meteorological event that caused a record highest rainfall in Mumbai. Curr Sci 90(10):1344–1362
Krishnamurthy V, Ajayamohan RS (2010) Composite structure of monsoon low-pressure systems and its relation to Indian rainfall. J Clim 23(16):4285–4305
Krishnamurthy V, Shukla J (2007) Intraseasonal and seasonally persisting patterns of Indian monsoon rainfall. J Clim 20(1):3–20
Krishnamurti TN, Hawkins RS (1970) Mid-tropospheric cyclones of the southwest monsoon. J Appl Meteorol 9(3):442–458
Kumar A, Dudhia J, Rotunno R, Niyogi D, Mohanty UC (2008) Analysis of the 26 July 2005 heavy rain event over Mumbai, India using the Weather Research and Forecasting (WRF) model. Quat J R Meteo Soc 134(636):1897–1910
Litta AJ, Chakrapani B, Mohankumar K (2007) Mesoscale simulation of an extreme rainfall event over Mumbai, India, using a high-resolution MM5 model. Meteorol Appl 14:291–295
Maity S, Satyanarayana ANV, Mandal M, Nayak S (2017) Performance evaluation of land surface models and cumulus convection schemes in the simulation of Indian summer monsoon using a regional climate model. Atmos Res 197:21–41
Maharana P, Dimri AP (2016) Study of intraseasonal variability of Indian summer monsoon using a regional climate model. Clim Dyn 46:1043–1064
Miller FR, Keshavamurthy RN (1967) Structure of an Arabian Sea Summer Monsoon System, International Indian Ocean Expedition. Meteorol Monogr 1:94
Mishra V, Aaadhar S, Shah H, Kumar R, Pattanaik DR, Tiwari AD (2018) The Kerala flood of 2018: combined impact of extreme rainfall and reservoir storage. Hydrol Earth Syst Sci Discuss. https://doi.org/10.5194/hess-2018-480
Mohanty UC, Routray A, Osuri KK, Prasad SK (2012) A study on simulation of heavy rainfall events over Indian region with ARW-3DVAR modeling system. Pure Appl Geophys 169(3):381–399
Mohanty MR, Sinha P, Maurya RKS, Mohanty UC (2019) Moisture flux adjustments in RegCM4 for improved simulation of Indian summer monsoon precipitation. Clim Dyn 52:7049–7069
Ngo-Duc T et al (2017) Performance evaluation of RegCM4 in simulating extreme rainfall and temperature indices over the CORDEX-Southeast Asia region. Int J Climatol 37(3):1634–1647
Nikumbh AC, Chakraborty A, Bhat GS, Frierson DM (2020) Large-scale extreme rainfall producing synoptic systems of the Indian summer monsoon. Geophys Res Lett. https://doi.org/10.1002/essoar.10502887.1
O'Gorman PA (2015) Precipitation extremes under climate change. Curr Clim Change Rep 1(2):49–59
Ogura Y, Yoshizaki M (1988) Numerical study of orographic-convective precipitation over the eastern Arabian Sea and the Ghat Mountains during the summer monsoon. J Atmos Sci 45(15):2097–2122

Pal JS, Giorgi F, Bi X, Elguindi N, Solmon F, Gao X, Ashfaq M (2007) Regional climate modeling for the developing world: the ICTP RegCM3 and RegCNET. Bull Am Meteorol Soc 88(9):1395–1410

Pfahl S, O'Gorman PA, Fischer EM (2017) Understanding the regional pattern of projected future changes in extreme precipitation. Nat Clim Change 7(6):423–427

Pradhan PK, Dasamsetti S, Ramakrishna SSVS, Dodla VBR, Panda J (2015) Mesoscale simulation of off-shore trough and mid-tropospheric cyclone associated with heavy rainfall along the West Coast of India using ARMEX Reanalysis. Int J Earth Atmos Sci 2(1):01–15

Rajeevan M, Bhate J, Kale JD, Lal B (2006) High resolution daily gridded rainfall data for the Indian region: analysis of break and active. Curr Sci 91(3):296–306

Rakhecha PR, Kulkarni AK, Mandal BN, Deshpande NR (1990) Homogeneous zones of heavy rainfall of 1-day duration over India. Theor Appl Climatol 41(4):213–219

Revadekar JV, Preethi B (2012) Statistical analysis of the relationship between summer monsoon precipitation extremes and food grain yield over India. Int J Climatol 32(3):419–429

Reynolds RW, Smith TM, Liu C, Chelton DB, Casey KS, Schlax MG (2007) Daily high-resolution-blended analyses for sea surface temperature. J Clim 20:5473–5496

Roxy MK, Ghosh S, Pathak A, Athulya R, Mujumdar M, Murtugudde R, Rajeevan M (2017) A threefold rise in widespread extreme rain events over central India. Nat Commun 8(1):1–11

Saeed S, Munir Sheikh M, Faisal S (2006) Simulations of 1992 flood in river Jhelum using high resolution regional climate model, précis to study the underlying physical processes involved in the extreme precipitation event. Pak J Meteorol 3(6):35–55

Saeed S, Liu Y, Rasul G (2011) Multiyear hindcast simulations of summer monsoon over South Asia using a nested regional climate model—BCC_RegCM1.0. Theor Appl Climatol 103(1):249–264

Sahany S, Venugopal V, Nanjundiah RS (2010) The 26 July 2005 heavy rainfall event over Mumbai: numerical modeling aspects. Meteorol Atmos Phys 109(3–4):115–128

Schwartz BE, Chappell CF, Togstad WE, Zhong XP (1990) The Minneapolis flash flood: meteorological analysis and operational response. Weather Forec 5(1):3–21

Shahi NK, Das S, Ghosh S, Maharana P, Rai S (2021) Projected changes in the mean and intra-seasonal variability of the Indian summer monsoon in the RegCM CORDEX-CORE simulations under higher warming conditions. Clim Dyn 57:1489–1506

Shyamala B, Bhadram CVV (2006) Impact of mesoscale–synoptic scale interactions on the Mumbai historical rain event during 26–27 July 2005. Curr Sci 91(25):1649–1654

Sikka DR, Rao PS (2008) The use and performance of mesoscale models over the Indian region for two high-impact events. Nat Hazards 44(3):353–372

Simmons A, Uppala S, Dee D, Kobayashi S (2007) ERA Interim: New ECMWF reanalysis products from 1989 onwards. ECMWF Newsl 110:1–11

Simpkins G (2017) Hydroclimate: Extreme rain in India. Nat Clim Change 7(11):760

Singh D, Tsiang M, Rajaratnam B, Diffenbaugh NS (2014) Observed changes in extreme wet and dry spells during the South Asian summer monsoon season. Nat Clim Change 4(6):456–461

Sinha P, Mohanty UC, Kar SC, Dash SK, Kumari S (2013) Sensitivity of the GCM driven summer monsoon simulations to cumulus parameterization schemes in nested RegCM3. Theor Appl Climatol 112:285–306

Sinha P, Mohanty UC, Kar SC, Kumari S (2014) Role of the Himalayan orography in simulation of the Indian summer monsoon using RegCM3. Pure Appl Geophys 171:1385–1407

Sinha P, Maurya RKS, Mohanty MR, Mohanty UC (2019) Inter-comparison and evaluation of mixed-convection schemes in RegCM4 for Indian summer monsoon simulation. Atmos Res 215:239–252

Smith RB, Durran D, Grossman R (1985) Comment on Interaction of low-level flow with the Western Ghat Mountains and offshore convection in the summer monsoon. Mon Weather Rev 113(12):2176–2181

Soman MK, Kumar KK (1990) Some aspects of daily rainfall distribution over India during the south-west monsoon season. Int J Climatol 10(3):299–311

Swain M, Sinha P, Pattanayak S, Guhathakurta P, Mohanty UC (2019a) Characteristics of observed rainfall over Odisha: an extreme vulnerable zone in the east coast of India. Theor Appl Climatol. https://doi.org/10.1007/s00704-019-02983-w

Swain M, Sinha P, Mohanty UC, Pattnaik S (2019b) Dominant large-scale parameters responsible for diverse extreme rainfall events over vulnerable Odisha state in India. Clim Dyn 53:6629–6644

Taylor KE (2001) Summarizing multiple aspects of model performance in a single diagram. J Geophys Res 106(D7):7183–7192

Tiedtke M (1989) A comprehensive mass flux scheme for cumulus parameterization in large-scale models. Mon Weather Rev 117(8):1779–1800

Turner AG, Annamalai H (2012) Climate change and the South Asian summer monsoon. Nat Clim Change 2(8):587–595

Vaidya SS, Kulkarni JR (2007) Simulation of heavy precipitation over Santacruz, Mumbai on 26 July 2005, using Mesoscale model. Meteorol Atmos Phys 98:55–66

Verma S, Bhatla R (2021) Performance of RegCM4 for dynamically downscaling of El Nino/La Nina events during Southwest Monsoon over India and its regions. Earth Space Sci. https://doi.org/10.1029/2020EA001474

Verma S, Bhatla R, Ghosh S, Sinha P, Mall RK, Pant M (2021) Spatio-temporal variability of summer monsoon surface air temperature over India and its regions using Regional Climate Model. Int J Climatol. https://doi.org/10.1002/joc.7155

Winkler JA (1988) Climatological characteristics of summertime extreme rainstorms in Minnesota. Ann Am Assoc Geogr 78(1):57–73

Xue Y, Janjic Z, Dudhia J, Vasic R, De Sales F (2014) A review on regional dynamical downscaling in intraseasonal to seasonal simulation/prediction and major factors that affect downscaling ability. Atmos Res 147:68–85